Title

Impaired Hypercarbic and Hypoxic Responses from Developmental Loss of Cerebellar Purkinje Neurons: Implications for Sudden Infant Death Syndrome

Journal

The Cerebellum, 13(6)

ISSN

1473-4222

Authors

Calton, M
Dickson, P
Harper, RM
et al.

Publication Date

2014-12-01

DOI

10.1007/s12311-014-0592-1

Peer reviewed

HHS Public Access

Author manuscript

Cerebellum. Author manuscript; available in PMC 2015 December 01.

Published in final edited form as:

Cerebellum. 2014 December ; 13(6): 739–750. doi:10.1007/s12311-014-0592-1.

Impaired hypercarbic and hypoxic responses from developmental loss of cerebellar Purkinje neurons: Implications for sudden infant death syndrome

M. Calton[1], **P. Dickson**[2], **R.M. Harper**[3], **D. Goldowitz**[4], and **G. Mittleman**[5]

[1] Department of Psychology, The University of Memphis, 400 Innovation Drive, Memphis, TN 38152

[2] The Jackson Laboratory, 600 Main Street, Bar Harbor, ME 04609

[3] David Geffen School of Medicine, UCLA Neurobiology, 695 Charles Young Drive South BOX 951763, Suite 78-113 BRI, Los Angeles, CA 90095

[4] Centre for Molecular Medicine and Therapeutics, University of British Columbia, 950 West 28th Avenue, Vancouver, BC, V5Z 4H4 Canada

[5] Department of Psychological Science, Ball State University, NQ 104, Muncie, IN, 47306 USA

Abstract

Impaired responsivity to hypercapnia or hypoxia is commonly considered a mechanism of failure in Sudden Infant Death Syndrome (SIDS). The search for deficient brain structures mediating flawed chemosensitivity typically focuses on medullary regions; however, a network that includes Purkinje cells of the cerebellar cortex and its associated cerebellar nuclei also helps mediate responses to CO_2 and O_2 challenges, and assists integration of cardiovascular and respiratory interactions. Although cerebellar nuclei contributions to chemoreceptor challenges in adult models are well described, Purkinje cell roles in developing models are unclear. We used a model of developmental cerebellar Purkinje cell loss to determine if such loss influenced compensatory ventilatory responses to hypercapnic and hypoxic challenges. Twenty-four *Lurcher* mutant mice and wildtype controls were sequentially exposed to 2% increases in CO_2 (0%-8%), or 2% reductions in O_2 (21%-13%) over four minutes, with return to room air (21% O_2 / 79% N2 / 0% CO_2) between each exposure. Whole-body plethysmography was used to continuously monitor tidal volume (TV) and breath frequency (*f*). Increased *f* to hypercapnia was significantly lower in Mutants, slower to initiate, and markedly lower in compensatory periods, except for very high (8%) CO_2 levels. The magnitude of TV changes to increasing CO_2 appeared smaller in Mutants, but only approached significance. Smaller, but significant differences emerged in response to hypoxia, with Mutants showing smaller TV when initially exposed to reduced O_2, and lower *f* following exposure to 17% O_2. Since cerebellar neuropathology appears in SIDS victims, developmental cerebellar neuropathology may contribute to SIDS vulnerability.

Communicating Author: Guy Mittleman, gmittleman@BSU.EDU, Telephone: 765-285-1695, Fax: 765-285-1702.

Conflicts of Interest: none

Keywords

cerebellum; sudden infant death; autism spectrum disorders; Lurcher; respiration

Introduction

Sudden Infant Death Syndrome (SIDS) is defined as the unexplained death during sleep of an otherwise healthy infant under the age of one year for which no apparent cause is revealed by autopsy or death scene investigation [1, 2]. SIDS is a principal cause of death in children in developed countries, and accounts for 22% of all infant deaths annually in the United States [3, 4]. With the advent of programs to encourage the supine sleeping position, pacifier use, and parental tobacco avoidance, the number of infants who succumb to SIDS has declined [5]. However, SIDS remains a leading cause of death in infants, suggesting that these behavioral changes, implemented to increase available O_2 to the infant, or decrease environmental CO_2 levels, only partially counteract vulnerability to this disorder [2-6].

The current consensus is that SIDS results from the intersection of several simultaneously occurring factors, including the presence of not-yet-described brain abnormalities, a critical developmental stage of the fatal event, and an inability to compensate for, and/or recover from, exogenous cardiovascular or respiratory stressors [2, 6-8]. Cardiac and breathing systems closely interact, with alterations in one system inducing changes in the other. Thus, an inappropriate respiratory response to a challenge can lead to an unsuitable cardiovascular response, possibly even hypotension and reduced perfusion, with significant consequences for survival.

Normal, relaxed (eupneic) breathing depends on a well-described set of central and peripheral processes which sense absorbed oxygen (O_2), carbon dioxide (CO_2) and mechanical distortions of the lung and thoracic wall, and integrate those signals to regulate homeostasis [9]. Other afferents from the cardiovascular system contribute to normal breathing patterns, and breathing, in turn, leads to an acceleration and deceleration of heart rate with inspiration and expiration; both systems depend on pontine, medullary and cerebellar structures for that integration[10-12]. When challenged with increased CO_2 levels or reduced O_2, the phenotypic respiratory response in both animals and humans is to increase the total volume of air breathed in one minute, (minute ventilation, MV), to compensate for rising blood CO_2 levels in an effort to maintain homeostasis. Minute ventilation is further comprised of two components: the volume of air inhaled in each breath (Tidal Volume, TV) and the number of breaths per minute, (breath frequency, f) [Knickmeyer-27; Moosavi-40; Sherwood-9]. The ventilatory responses to hypercapnia and hypoxia can provide indications of stressed breathing. Furthermore, with extreme perturbation of respiratory or cardiovascular systems, “stressed breathing,” or exaggerated changes in blood pressure require particular structures to provide compensatory responses to such challenges. Those structures include sites regulating eupneic breathing, but may recruit other areas to overcome extreme, or stressed challenges [13-15].

Cerebellar structures appear to play significant roles in extreme challenges or stressed breathing. Complete cerebellectomy has little influence on eupneic breathing, but markedly

alters breathing responses to exaggerated reductions in O_2 and increased CO_2 [16, 17]. Cerebellar influences on stressed breathing occur via output through the cerebellar nuclei, including the rostral fastigial, lateral, and interposed nuclei (FNr, LCN, IN), since ablation of these nuclei alters the response to increases in CO_2 [18]. Thus, the cerebellum significantly contributes to the compensation to, and recovery from, exogenous respiratory stressors [15, 18-20]. Although neuropathology appears in both brainstem respiratory regulatory areas and the cerebellum in SIDS victims, it is unclear if this damage precedes the fatal event, or results from hypoxemia, hypercarbia or cardiovascular changes that occur prior to a SIDS death [21-24].

SIDS occurs within a remarkably narrow developmental period, principally within the 2^{nd} to 4^{th} month of life, and typically within the first year [25]. During that first year, brain size increases to nearly 70% of adult size, with the greatest growth occurring in the cerebellum [26-28]. Postnatal maturation of the cerebellar cortex is delayed in SIDS victims, relative to age-matched controls, suggesting a developmental contribution to failure in addition to an underlying brain pathology [29].

The third assumption in the SIDS consensus is that death results from a failure to respond to, compensate for, and/or recover from an exogenous respiratory or cardiovascular challenge. To assess SIDS susceptibility, the most frequently investigated challenges involve exposure to excessive CO_2 (hypercapnia) or reduced O_2 (hypoxia), and such evaluations typically are carried out during sleep and wakefulness [30], while cardiovascular challenges typically include tilt testing for respiratory, heart rate and blood pressure responses [31, 32].

Given the role of cerebellar structures in responding to extreme respiratory challenges, and evidence of excessive apoptosis of cerebellar Purkinje cells in SIDS victims [33], we propose that a developmental model of mouse cerebellar injury should show impaired compensatory responses to exaggerated ventilatory challenges. We used *Lurcher* mutant mice, which lose nearly all their cerebellar Purkinje cells during the first four weeks of life due to a spontaneous gain-of-function mutation in the delta-2 glutamate receptor gene (Grid2) [34, 35], and then measured respiratory responses during conditions of hypercapnia and hypoxia. Purkinje cells comprise the sole output pathway of the cerebellar cortex, and project through the FNr, LCN, and IN to multiple pathways to the medulla and other brain areas [36, 37]. We hypothesized that *Lurcher* mutant mice would show deficits in responding to and recovering from acute CO_2 and O_2 challenges, compared to littermate, wildtype mice with normal numbers of cerebellar Purkinje cells.

METHODS

Animals

Mice were bred and housed in the Animal Care Facility of the Department of Psychology at the University of Memphis. They were maintained in a temperature-controlled environment (21±1°C) on a 12:12 light-dark cycle (lights on at 0700), and given free access to food and water. Original *Lurcher* (#001046) breeders were purchased from The Jackson Laboratory (Bar Harbor, Maine). All experiments were approved by the University of Memphis

Institutional Animal Care and Use Committee, and conducted in accordance with the National Institutes of Health Guidelines for the Care and Use of Laboratory Animals.

Breeding

The breeding of *Lurcher* mice (Lc/+) entailed filial pairing of a non-ataxic female wildtype (WT; B6CBACa $A^{w\text{-}J}$/A-$Grid2^{+}$) with a mutant ataxic male heterozygous for the *Lurcher* spontaneous mutation (Lc/+; B6CBACa $A^{w\text{-}J}$/A-$Grid2^{Lc}$). This breeding strategy produced litters composed of both heterozygous Lc/+ and WT mice. The Lc/+ mouse is phenotypically distinguishable from wildtype littermates as early as postnatal day 12 (PND 12) with cerebellar signs, including an ataxic gait, which permits the non-invasive differentiation of Lc/+ mice from their non-ataxic WT littermates [35].

Animals were weaned at PND 25 +/− 4 days and sibling-housed in groups of 3-5 in ventilated polystyrene cages. The subjects consisted of 24 male mice (12 LC+ and 12 WT) that were PND 60 at testing onset, and weighed 20g (+/−3g). To rule out potential litter effects, only one mouse of each genotype from each litter was used for this study.

Whole Body Plethysmography

Data were collected using a whole body plethysmography system (WBP; Emka Technologies; Falls Church, VA, USA). Animals were placed, unrestrained, into a cylindrical Plexiglas chamber (volume ≈ 450ml). Three Allicat flow control modules supplied gas to the chamber (at 1.0L/min), each calibrated for a separate gas (CO_2 and O_2: MC-200SCCM-D/10M, N_2: MC-1SLPM-D/10M, Tucson, AZ, USA). Gas mixtures were controlled using an Allicat RS32 multidrop box (model BB9; Tucson, AZ, USA), that received input from a standard desktop computer via Emka Technologies iOX2 software (2013). A transducer was mounted to the WBP, which converted pressure differentials in the chamber into electrical signals that were then transmitted to, and interpreted by the software. An outflow ventilation pump (Emka Technologies; Falls Church, VA, USA) was connected to the WBP to ensure constant removal of exhaled CO_2 at 0.8L/min to prevent accumulation of this gas.

Procedure

Mice were weighed prior to placement in the chamber. The experimental room temperature (22°C +/− 3°C), and humidity (20% +/−5%), were monitored daily to ensure stability throughout the study. Three separate programs were used to assess the subjects' respiratory responses at baseline (normal room air; 21% O_2, 0% CO_2 and 79% N_2), and under conditions of increased CO_2 (hypercapnia) or reduced O_2, (hypoxia). Mice were randomly assigned to either the hypercapnia or hypoxia condition on PND 60, and the second condition followed on PND 61. Each test day began with a 10-minute habituation period, followed by a four minute exposure to baseline (Room Air) period. Exposure to hypercapnic or hypoxic conditions followed baseline. Mice were exposed to continuously flowing room air at all times (0.8-1.0 L/m), during the habituation and baseline period.

Baseline—After the 10 minute habituation period, dependent variables, including tidal volume (TV; ml, the volume of inhaled air in one breath), and breath frequency (*f* , the

number of breaths per minute), were continuously recorded while the mice were exposed to room air for a total of four minutes (21% O_2, 0% CO_2, 79% N).

Hypercapnia—The entire hypercapnia program was 52 minutes duration, and consisted of one beginning baseline (four minutes) measured as described above, followed by four sequential challenges where CO_2 was progressively increased from 2%, 4%, 6%, and 8%, (21% O_2, N_2 on balance). Each of the four CO_2 challenges consisted of a two-minute chamber fill period (the time required for the WBP to achieve the desired gas percentages), followed by a four-minute exposure. To minimize discomfort of the animals, between each challenge, the program returned to room air (again, including a two-minute chamber refill period and a four-minute recovery period). At termination of the final CO_2 exposure (8%), and return to room air, the mouse was removed from the chamber.

Hypoxia—Similar procedures were followed for hypoxia testing, with the exception that following the initial baseline period (four minutes), O_2 was progressively reduced to 19%, 17%, 15%, and 13%, (0% CO_2, N_2 on balance). As above, reduced O_2 exposures were separated by room air chamber refills and recovery periods. Thus, the duration of hypoxia testing was also 52 minutes.

Variables and Data Analysis

The dependent variables in all conditions were TV and *f*. Both measures were averaged over 10-s intervals during baseline, hypercapnia and hypoxia testing.

Baseline—The two baselines collected prior to the hypercapnia and hypoxia conditions were compared using repeated measures analysis of variance (RMANOVA). Measures of TV and *f* were separately analyzed. In both analyses, Genotype (Lc/+ and WT) served as the between-subjects factor, while Baseline (1 and 2), and Interval (24, 10-second intervals) served as the within-subjects factors.

Hypercapnia and Hypoxia—For each condition, separate omnibus RMANOVAs were initially performed on TV and *f*. Genotype again served as the between-subject factor. Within-subjects factors included four levels of gas exposure (Hypercapnia 2%, 4%, 6%, and 8% CO_2, or Hypoxia, 19%, 17%, 15%, and 13% O_2). Additionally, each gas exposure was subdivided into two-minute time blocks, such that the blocks corresponded to chamber fill, gas exposure 1, gas exposure 2, chamber refill (return to room air), recovery 1, and recovery 2. The two-minute blocks were additionally divided into twelve, 10-second intervals to accurately track moment-to-moment changes in TV and *f*. Therefore, the omnibus analysis became a 2 (Genotype) × 4 (Gas Exposure) × 6 (Time Blocks) × 12 (10-second Interval) mixed design. Depending on the results of the omnibus RMANOVAs, additional main-effects tests were used to analyze interaction effects.

RESULTS

An independent samples t-test revealed no significant difference in body weight between the two genotypes (t (22) = −1.629, p = .118).

Baseline

Tidal volume did not differ significantly between *Lurcher* and WT mice across the baseline exposures from room air. Figure 1 (a) shows this variable, averaged over 10 s time intervals in Lc/+ and WT mice (Baseline, F (1, 22) = 1.15, p = ns). RMANOVA also indicated that TV in mice of both genotypes did not differ significantly (Genotype, F (1, 22) = 0.72, p = ns). Thus, average TV in Lc/+ and WT mice was, respectively, 0.162 (*SE* = 0.011), 0.171 (*SE* = 0.011). TV remained constant between groups during exposure to room air (Group × Interval, F (23, 506) = 1.20, p = ns).

Breath frequency did not differ significantly across the two baselines, and was averaged across exposures (Baseline, F (1, 22) = 3.64, p = ns). As shown in Figure 1 (b), breath frequency averaged 357.8 (*SE* = 10.14) in LC+ mice and 358.6 (*SE* = 10.14) in WT mice over baseline. RMANOVA confirmed that both genotypes had equivalent breath frequency (Group, F (1, 22) = 0.01, p = ns), which remained stable between groups over baseline intervals (Group × Interval, F (23, 506) = 1.25, p = ns).

Hypercapnia

Figure 2 (a, b, c, d) illustrates the increase in tidal volume that occurred as a function of CO_2, rising from 2% to 8% in LC+ and WT mice. Two patterns of change appeared: first, during time blocks corresponding to increased CO_2 concentration (Exposure), TV consistently increased in both genotypes, and then declined when gas composition returned to room air (Refill and Recovery; Time Block F (5, 110) = 25.97, $p < .001$). Secondly, as CO_2 concentration increased from 2 to 8%, the magnitude of TV progressively increased (Gas Exposure × Time Block, F (15, 330) = 19.18, $p < .001$). Although LC+ mice consistently showed smaller increases in TV during periods of increased CO_2 concentration, the omnibus RMANOVA indicated that genotype-related differences only approached significance (Genotype, F (1, 22) = 2.14, p = 0.16), and additional interaction effects involving genotype were also not significant.

Figure 2 (e, f, g, h) shows the effects of increasing concentrations of CO_2 on breath frequency. Two patterns of change were also apparent. Regardless of CO_2 level, breath frequency increased significantly during CO_2 exposure, and declined when gas composition returned to room air (Refill and Recovery; Time Block F (5, 110) = 15.48, $p < .001$). When considered across different levels of CO_2, small but significant reductions in breath frequency in both groups occurred (Gas exposure, F (3,66) = 6.48, $p < .001$). Thus, in both genotypes at 2% CO_2, breath frequency averaged 344.38 (*SE* = 22.86), but was reduced to 316.50 (*SE* = 5.02), 309.59 (*SE* = 11.96) and 315.65 (*SE* = 5.88), as CO_2 levels increased respectively to 4, 6 and 8%. RMANOVA indicated that the two genotypes responded significantly differently at all CO_2 concentrations (Genotype, F (1, 22) = 7.85, p = 0.01), that varied as a function of time block (Genotype × Time Block, F (5, 110) = 2.34, $p <$ 0.05). Simple main-effects tests were used to specify the genotype-related differences at each time block, and are shown in Figure 3 a. When considered across CO_2 concentrations, LC+ animals consistently exhibited lower breath frequencies than WT controls during chamber fill, gas exposure 1, gas exposure 2, chamber refill (return to room air), recovery 1 and recovery 2. These genotypic differences were significant in all time blocks, with the

exception of the initial exposure to increased CO_2 (exposure 1). During this time block, genotypic differences only approached significance (Exposure 1, F (1, 22) = 2.82, p = 0.11).

The simple main effects tests also indicated that during the recovery 1 condition, genotypes differed as a function of CO_2 concentration (Genotype × Gas Exposure, F (3,66) =2.75, p = .05). Figure 3 b shows the results of these additional simple main effects tests restricted to each CO_2 concentration during recovery 1, with Lc/+ mice showing significantly lower breath frequency than wildtype controls following exposure to 2% (F (1,22) = 11.98, p<.01) and 4 % CO_2 (F (1,22) = 4.23, p =.05).

Hypoxia

Figure 4 (a, b, c, d) shows the effects of progressively decreasing O_2 concentrations on tidal volume. As O_2 decreased from 19 to 13%, TV progressively declined. Thus, for both genotypes, TV averaged 0.155 ml (SE = 0.011) at 19% O_2, which progressively declined to 0.147 (SE = 0.004), 0.136 (SE = 0.007) and 0.135 (SE = 0.008) as O_2 concentration was reduced to 17, 15 and 13% (Gas Exposure F (3,66) = 26.77, p < .001). The omnibus RMANOVA indicated that, when considered across reductions in O_2 levels, small, but significant differences appeared in TV between genotypes (Genotype × Time Block × Interval, F (55, 1210) = 1.61, p = 0.003). Follow-up analyses revealed that during chamber fill, LC+ mice had significantly smaller tidal volumes than WT controls (Fill, F (11, 242) = 2.45, p = 0.007). As shown in Figure 4, this genotype-related difference occurred predominantly at O_2 concentrations of 13 and 15%.

Figure 4 (e, f, g, h) indicates the effects of differing levels of hypoxia on breath frequency. RMANOVA indicated that in both groups, O_2 reductions resulted in a progressive decrease in average breath frequency from 326.15 (SE = 55.32) at 19% O_2 to 276.55 (SE = 5.73), 238.72 (SE = 32.11) and 241.88 (SE = 28.94) at respectively, 17, 15 and 13% O_2 (Gas Exposure, F (3, 66) = 36.82, p < 0.001). Genotype-related differences appeared in how LC+ and WT mice responded to reduced O_2 (Genotype × Gas Exposure, F (3, 66) = 2.91, p = 0.04; Genotype × Time Block × Interval, F (55, 1210) = 1.51, p = 0.01). Follow-up analyses revealed significant differences between genotypes at exposure to 17% O_2 (17%, F (1, 22) = 5.34, p = 0.03). As shown in Figure 4 (panel f), Lc/+ mice had significantly lower breath frequencies during chamber refill and recovery following exposure to 17% O_2.

Discussion

At baseline, LC/+ mice and wildtype controls exhibited similar responses to normal room air in both TV and *f*, indicating eupneic breathing in both groups was equivalent (Fig 1). As others have shown [16, 17], this finding provides additional support for the hypothesis that cerebellar damage exerts little influence on eupneic breathing. Additionally, these results specifically demonstrate that developmental loss of cerebellar Purkinje cells has little influence on eupneic respiration.

However, the patterns for ventilatory challenges substantially differed between groups. *Lurcher* mutant mice exhibited significant deficits in compensating for increased CO_2 in comparison to WT mice (Fig. 2). Both genotypes increased TV during exposure to increased

CO_2 levels, and this increase in TV was magnified as CO_2 concentration increased from 2 to 8%. Although TV was consistently lower in LC+ mice, this difference only approached significance.

Breath frequency increased with exposure to increased CO_2 concentrations, and then declined upon re-exposure to room air in both genotypes (Fig. 2 & 3). However, in Lurcher mice, the decline was much more rapid, except at extreme levels of hypercapnia (6% and 8%). Together with the TV changes, this finding indicates that both groups showed initial typical compensatory responses to increased CO_2 levels [9, 27, 38-40]. Importantly, when considered across all levels of increased CO_2, *f* was consistently lower in Lc+ mice when compared to wildtype controls (Fig. 3). This genotype-related difference in *f* was significant during initial chamber fill while CO_2 levels were rising, during the second two minutes of exposure to increased CO_2, and throughout the refill to normal room air, and while normal room air was maintained.

These response patterns indicate that Lc/+ mice were impaired in responding to multiple aspects of this CO_2 challenge. Specifically, the significantly lowered response to increasing concentrations of CO_2 during the initial chamber fill indicates that Lc/+ mice were slower to initiate a compensatory increase in *f* in response to increasing hypercapnia. That the genotypes did not differ significantly during the first 2 minutes of exposure to increased CO_2 shows that Lc/+ mice ultimately did initiate a compensatory response to the CO_2 challenge. However, Lc/+ mice then failed to maintain this compensatory increase during the second two minutes of exposure. The inability to maintain the compensatory response may indicate that Lc/+ mice were relatively insensitive to rising CO_2 levels. The failure to maintain compensation presumably lead to higher blood levels of CO_2 in LC+ mice than those of control [9, 12]. Thus, the subsequent genotype-related differences in *f* that occurred during chamber refill and maintenance with room air may additionally represent an inability to eliminate the increased blood levels of CO_2. The patterns of respiratory rates at very high levels of CO_2 (6 % and 8%) were similar in both groups, likely resulting from a ceiling effect for CO_2.

When exposed to hypoxia, both genotypes exhibited a gradual reduction in TV and *f* as O_2 concentration decreased (Fig. 4). It should be noted that both the magnitude of changes in TV and *f*, as well as the pattern of ventilatory decline observed in both genotypes can be considered to be relatively typical. Hypoxia, especially when O_2 levels do not decline below 10%, elicits a much less robust response than hypercapnia, as the respiratory and cardiovascular systems tend to be more receptive to changes in CO_2 than O_2 [41, 42]. Additionally, the hypoxic ventilatory decline found across the O_2 challenges in both genotypes is likely related to their genetic background, since that pattern is a typical response in C57BL/6 mice [43, 44].

Genotype-related differences were relatively small and infrequent during the hypoxic challenges. At 17% and 15% O_2, during, respectively, the return to room air (17% O_2) and while the chamber was refilling with 15% O_2, Lc/+ mice had significantly lower *f* than wildtype controls. Thus, Lc/+ mice may have exhibited an impaired ability to recover from moderately reduced O_2 in comparison to WT mice.

The current results implicating cerebellar Purkinje cell loss in the differential reduction in responsiveness to hypercapnic conditions significantly differ from those earlier reported in another animal model of Purkinje cell degeneration. In Shaker mutant rats that exhibit varying levels of cerebellar Purkinje cell loss which begins seven weeks after birth, breath frequency during hypercapnia is augmented, rather than reduced [45, 46]. Aside from species-related differences, Shaker mutant rats also differ from *Lurcher* mutants in both the temporal and spatial patterns of Purkinje cell loss. Shaker mutant rats comprise two groups, mild and strong, that differentially exhibit hereditary cerebellar Purkinje cell loss [47]. The mild Shaker group is characterized behaviorally by ataxic gait, and exhibits cerebellar Purkinje cell loss that occurs randomly, primarily in the anterior lobe, begins by PND 42 to 49, and culminates approximately by PND 90. The “strong shaker” is characterized behaviorally by both ataxic gait and severe body tremors, and additionally exhibits near-complete cerebellar Purkinje cell loss in the anterior lobe that occurs by PND 90. Accompanying the early anterior lobe loss, Purkinje cells in the posterior lobe (lobules VIIb, VIII, IXa-c) continue to degenerate throughout the life of this model [45, 47].

Lurcher mutants, in contrast, exhibit global loss of cerebellar Purkinje cells that begins almost immediately after birth as a result of spontaneous apoptosis, with nearly 100% Purkinje cell loss in the cerebellar cortex by PND 28 [35, 45]. The combination of differences in the topography and timing of Purkinje cell loss between Lc/+ mice and Shaker mutant rats indicates that interpretation of the role of developmental cerebellar damage on stressed breathing is complex, and the relationship between cerebellar Purkinje cell loss and the response to hypercapnia is something other than a simple correlation between Purkinje cell number and respiratory response. Thus, the differences in outcomes highlight the need for further investigation of the effects of cerebellar Purkinje cell loss and challenged breathing.

A number of potential mechanisms may underly the Lc/+ mice deficits in respiratory compensatory behaviors in response to hypercapnia, and to a lesser degree, hypoxia. It appears unlikely that these differences can be attributed to peripheral mechanisms. Diaphragm muscles in Lc/+ mice have been reported to be *more* fatigue resistant than those of WT mice, which suggests that reduced muscle capability of the mutants does not play a role [48]. Additionally, a motor deficit in Lc/+ mice appears unlikely, as these animals were capable of achieving appropriate levels of TV and *f*. Thus, for example, TV in Lc/+ mice at 6% CO_2 matched or exceeded TV in wildtype mice at 4% CO_2 (Fig. 2 b, c).

A more likely explanation for the genotype-related differences found here involves one of the cerebellar nuclei, the fastigial nuclei. These nuclei facilitate compensatory respiratory responses to hypercapnia, and to a lesser extent, hypoxia [46, 49]. Cell body lesions of these nuclei had no effect on eupneic breathing, but markedly reduced respiratory responses to increased CO_2 [50]. Purkinje cells output through all the cerebellar nuclei, including the fastigial nuclei, together with a small projection to the vestibular nuclei [51]. In Lc/+ mice, as a function of loss of Purkinje cells and associated reductions in impulse traffic, the deep cerebellar nuclei exhibit a 60% reduction in volume [52]. It is reasonable to assume that shrinkage of the fastigial nuclei that occurs in Lc/+ mice likely also involves a loss of

chemosensitivity that could result in an inability to respond appropriately to hypercapnic conditions.

Schmahmann has advanced the concept that the cerebellum plays a homeostatic role, minimizing sensorimotor behavioral changes from baseline; when dysfunctional, the outcome is dysmetria in conventional motor regulation as well as other cerebellar regulatory aspects, including blood pressure (20), emotion, and cognitive processes [53]. The data here fit that hypothesis well. It could be argued that in the Lc/+ mice, this proposed dampener function is impaired, as much larger response variation from baseline appears to challenges and recovery from those challenges than in the WT controls. However, this possibility needs to be further examined, since cerebellar regulatory action during baseline conditions, rather than the challenged conditions, may follow different control patterns.

Although the current results implicate the loss of cerebellar Purkinje cells in the development of disordered breathing, the relationship between Purkinje cell loss and SIDS remains controversial. Cruz-Sanchez et al. (1997) found a delayed maturation of the external granule layer of the cerebellar cortex in SIDS victims, relative to age-matched controls [29]. However, two subsequent studies examining Purkinje cell density and volume in SIDS victims and controls reported no differences [54, 55]. While it is likely that the cerebellar area investigated, as well as methodology issues contribute to variability in these reports, the postmortem control brains used in these studies included those that succumbed from causes known to create hypoxemia prior to death, including strangulation, suffocation, carbon monoxide poisoning, and pneumonia. The cerebellum, and specifically, cerebellar Purkinje cells are highly sensitive to hypoxic insult, which results in cell death [45, 56-58]. Thus, the use of such control tissues may greatly reduce the likelihood of finding differences between SIDS victims and age-matched controls.

Disordered breathing is common across multiple disorders involving cerebellar pathology. For example, Chiari Type II malformations and Joubert Syndrome are respectively associated with herniation or hypoplasia of the cerebellar vermis, and both are characterized by sleep disordered breathing [59, 60]. This association is noteworthy, as the cerebellar vermis has long been recognized as significantly involved in cardiovascular regulation and respiratory response patterns to hypercapnia and air hunger [61-64]. Diffusion tensor imaging studies in children diagnosed with congenital central hypoventilation syndrome (CCHS), who typically hypoventilate during sleep and are insensitive to CO_2, have identified cerebellar abnormalities, including myelin alterations of the cerebellar vermis and cerebellar nuclei [65]. Additionally, persons with Fragile-X syndrome, the largest monogenic cause of autism, exhibit focal cerebellar Purkinje cell loss and Bergmann gliosis, and also show an increased incidence of sleep apnea, as well as an increased likelihood of giving birth to children who die from SIDS [66, 67].

Throughout autism spectrum disorders (ASD), cerebellar neuropathology, including cerebellar hypoplasia and reduced cerebellar Purkinje cell numbers are the most consistently reported neuropathologies [68-76]. Although there have been no systematic comparisons of the incidence of breathing disorders in ASD, sleep related disorders of stressed or challenged breathing, as well as SIDS appear in many clinical syndromes encompassed

within the ASD category. These disorders include phenylketonuria, Joubert syndrome, Fragile X, Angelman syndrome, Rett syndrome and Mobius syndrome [67, 77-82]. Although neuropathologic studies of some of these disorders are rare, they appear to involve varying types of cerebellar abnormalities that include extensive cerebellar neuron loss [83], agenesis or dysgenesis of the cerebellar vermis [84], focal cerebellar Purkinje cell loss and Bergmann gliosis [66], cerebellar atrophy [85], gliosis, hypoplasia and progressive atrophy in the cerebellum, including Purkinje cell loss [86, 87], and cerebellar hypoplasia [88, 89]. Although these disorders also show varying degrees of neuropathology in other brain areas, the common features linking all of these disorders are developmental cerebellar neuropathology, autistic symptomatology and sleep disordered breathing. The findings here indicate a need to further evaluate cerebellar pathology, more specifically Purkinje cell pathology, as a potential contributor to respiratory responses and compensation during stressed or challenged breathing. The developmental nature of some of the cerebellar pathologies, together with the importance on strategic breathing issues of concern in SIDS, make damage to that structure a major concern in that syndrome.

Funding and Acknowledgements

This project was made possible by NINDS grant 1R01NS063009.

References

1. Krous H, Bechwith B, Byard R, Rognum T, Bajanowski T, Corey T. Sudden infant death syndrome. Pediatrics. 2004; 114(1):234–8. [PubMed: 15231934]
2. Health NIoC. Development H. From cells to selves: targeting Sudden Infant Death Syndrome (SIDA): a strategic plan. National Institute of Child Health and Human Development; 2001.
3. Malloy MH, MacDorman M. Changes in the classification of sudden unexpected infant deaths: United States, 1992-2001. Pediatrics. 2005; 115(5):1247–53. doi: 10.1542/peds.2004-2188. [PubMed: 15867031]
4. Hauck FR, Tanabe KO. International trends in sudden infant death syndrome: stabilization of rates requires further action. Pediatrics. 2008; 122(3):660–6. doi: 10.1542/peds.2007-0135. [PubMed: 18762537]
5. Trachtenberg FL, Haas EA, Kinney HC, Stanley C, Krous HF. Risk factor changes for sudden infant death syndrome after initiation of Back-to-Sleep campaign. Pediatrics. 2012; 129(4):630–8. doi: 10.1542/peds.2011-1419. [PubMed: 22451703]
6. Moon RY, Horne RSC, Hauck FR. Sudden infant death syndrome. The Lancet. 2007; 370(9598): 1578–87. doi: 10.1016/s0140-6736(07)61662-6.
7. Guntheroth WG, Spiers PS. The triple risk hypotheses in sudden infant death syndrome. Pediatrics. 2002; 110(5):e64. doi: 10.1542/peds.110.5.e64. [PubMed: 12415070]
8. Bergman, AB.; Beckwith, JB.; Ray, CG. Sudden infant death syndrome: proceedings of the second international conference on causes of sudden death in infants; Seattle, Washington. University of Washington Press; 1969. 1970
9. Sherwood, L. Human physiology from cells to systems. 3. Wadsworth Pub. Co.; Belmont, CA: 1997. p. 753
10. Hilaire G, Dutschmann M. Foreword: respiratory rhythmogenesis. Respir Physiol Neurobiol. 2009; 168(1-2):1–3. doi: 10.1016/j.resp.2009.06.017. [PubMed: 19573628]
11. Spyer KM, Gourine AV. Chemosensory pathways in the brainstem controlling cardiorespiratory activity. Philos Trans R Soc Lond B Biol Sci. 2009; 364(1529):2603–10. doi: 10.1098/rstb.2009.0082. [PubMed: 19651660]
12. Alheid, GF.; McCrimmon, DR. Encyclopedia of Neuroscience. Springer; 2009. Anatomy and Function in the Respiratory Network; p. 110-22.

13. Onimaru H, Ikeda K, Kawakami K. Phox2b, RTN/pFRG neurons and respiratory rhythmogenesis. Respir Physiol Neurobiol. 2009; 168(1-2):13–8. doi: 10.1016/j.resp.2009.03.007. [PubMed: 19712902]
14. McCrimmon DR, Alheid GF. Capra, eupnea, dyspnea, apnea: respiratory rhythms and the pre-Botzinger complex in the goat. J Appl Physiol. 2004; 97(5):1618–9. doi: 10.1152/japplphysiol.00627.2004. [PubMed: 15475553]
15. Harper R. The cerebellum and respiratory control. Cerebellum. 2002; 1(1):1. [PubMed: 12879968]
16. Xu F, Frazier DT. Modulation of respiratory motor output by cerebellar deep nuclei in the rat. J Appl Physiol. 2000; 89(3):996–1004. [PubMed: 10956343]
17. Xu F, Owen J, Frazier DT. Hypoxic respiratory responses attenuated by ablation of the cerebellum or fastigial nuclei. J Appl Physiol. 1995; 79(4):1181–9. [PubMed: 8567560]
18. Xu F, Frazier DT. Role of the cerebellar deep nuclei in respiratory modulation. Cerebellum. 2002; 1(1):35–40. [PubMed: 12879972]
19. Lu L, Cao Y, Tokita K, Heck DH, Boughter JD Jr. Medial cerebellar nuclear projections and activity patterns link cerebellar output to orofacial and respiratory behavior. Front Neural Circuits. 2013; 7:56. doi: 10.3389/fncir.2013.00056. [PubMed: 23565078]
20. Harper RM, Kinney HC. Potential Mechanisms of Failure in the Sudden Infant Death Syndrome. Curr Pediatr Rev. 2010; 6(1):39–47. doi: 10.2174/157339610791317214. [PubMed: 22792083]
21. Kinney HC, Thach BT. The sudden infant death syndrome. N Engl J Med. 2009; 3618:795–805. [PubMed: 19692691]
22. Haouzi P. Initiating inspiration outside the medulla does produce eupneic breathing. J Appl Physiol. 2011; 110(3):854–6. doi: 10.1152/japplphysiol.00833.2010. [PubMed: 21030668]
23. Harper RM, Richard CA, Henderson LA, Macey PM, Macey KE. Structural mechanisms underlying autonomic reactions in pediatric arousal. Sleep Med. 2002:3, S53–S6.
24. Filiano J, Kinney H. A perspective on neuropathologic findings in victims of the sudden infant death syndrome: the triple-risk model. Neonatology. 1994; 65(3-4):194–7.
25. Beckwith JB. Defining the sudden infant death syndrome. Arch Pediatr Adolesc Med. 2003; 157(3):286–90. [PubMed: 12622679]
26. Tau GZ, Peterson BS. Normal development of brain circuits. Neuropsychopharmacology. 2010; 35(1):147–68. doi: 10.1038/npp.2009.115. [PubMed: 19794405]
27. Knickmeyer RC, Gouttard S, Kang C, Evans D, Wilber K, Smith JK, et al. A structural MRI study of human brain development from birth to 2 years. J Neurosci. 2008; 28(47):12176–82. doi: 10.1523/JNEUROSCI.3479-08.2008. [PubMed: 19020011]
28. Dekaban AS, Sadowsky D. Changes in brain weights during the span of human life: relation of brain weights to body heights and body weights. Ann Neurol. 1978; 4(4):345–56. [PubMed: 727739]
29. Cruz-Sanchez FF, Lucena J, Ascaso C, Tolosa E, Quintó L, Rossi ML. Cerebellar cortex delayed maturation in sudden infant death syndrome. J Neuropathol Exp Neurol. 1997; 56(4):340–6. [PubMed: 9100664]
30. Horne RS, Parslow PM, Harding R. Postnatal development of ventilatory and arousal responses to hypoxia in human infants. Respir Physiol Neurobiol. 2005; 149(1):257–71. [PubMed: 15876558]
31. Fifer WP, Greene M, Hurtado A, Myers MM. Cardiorespiratory responses to bidirectional tilts in infants. Early Hum Dev. 1999; 55(3):265–79. [PubMed: 10463790]
32. Yiallourou SR, Walker AM, Horne RS. Prone sleeping impairs circulatory control during sleep in healthy term infants: implications for SIDS. Sleep. 2008; 31(8):1139. [PubMed: 18714786]
33. Matturri L, Ottaviani G, Lavezzi AM. Maternal smoking and sudden infant death syndrome: epidemiological study related to pathology. Virchows Arch. 2006; 449(6):697–706. [PubMed: 17091255]
34. Caddy K, Biscoe T. Structural and quantitative studies on the normal C3H and Lurcher mutant mouse. Philos Trans R Soc Lond B Biol Sci. 1979:167–201. [PubMed: 41272]
35. Zuo J, De Jager PL, Takahashi KA, Jiang W, Linden DJ, Heintz N. Neurodegeneration in Lurcher mice caused by mutation in δ2 glutamate receptor gene. Nature. 1997; 388(6644):769–73. [PubMed: 9285588]

36. Harvey R, Napper R. Quantitatives studies on the mammalian cerebellum. Prog Neurobiol. 1991; 36(6):437–63. [PubMed: 1947173]
37. Napper R, Harvey R. Number of parallel fiber synapses on an individual Purkinje cell in the cerebellum of the rat. J Comp Neurol. 1988; 274(2):168–77. [PubMed: 3209740]
38. Frappell P, Lanthier C, Baudinette R, Mortola J. Metabolism and ventilation in acute hypoxia: a comparative analysis in small mammalian species. Am J Physiol Regul Integr Comp Physiol. 1992; 262(6):R1040–R6.
39. Tankersley CG, Fitzgerald RS, Kleeberger SR. Differential control of ventilation among inbred strains of mice. Am J Physiol Regul Integr Comp Physiol. 1994; 267(5):R1371–R7.
40. Moosavi SH, Golestanian E, Binks AP, Lansing RW, Brown R, Banzett RB. Hypoxic and hypercapnic drives to breathe generate equivalent levels of air hunger in humans. J Appl Physiol. 2003; 94(1):141–54. [PubMed: 12391041]
41. Fong AY. Postnatal changes in the cardiorespiratory response and ability to autoresuscitate from hypoxic and hypothermic exposure in mammals. Respir Physiol Neurobiol. 2010; 174(1-2):146–55. doi: 10.1016/j.resp.2010.08.012. [PubMed: 20797451]
42. Teppema LJ, Dahan A. The ventilatory response to hypoxia in mammals: mechanisms, measurement, and analysis. Physiol Rev. 2010; 90(2):675–754. [PubMed: 20393196]
43. Tankersley CG, Elston RC, Schnell AH. Genetic determinants of acute hypoxic ventilation: patterns of inheritance in mice. J Appl Physiol. 2000; 88(6):2310–8. [PubMed: 10846050]
44. Chai S, Gillombardo CB, Donovan L, Strohl KP. Morphological differences of the carotid body among C57/BL6 (B6), A/J, and CSS B6A1 mouse strains. Respir Physiol Neurobiol. 2011; 177(3): 265–72. doi: 10.1016/j.resp.2011.04.021. [PubMed: 21555000]
45. Sarna JR, Hawkes R. Patterned Purkinje cell death in the cerebellum. Prog Neurobiol. 2003; 70(6): 473–507. doi: 10.1016/s0301-0082(03)00114-x. [PubMed: 14568361]
46. Xu F, Zhou T, Frazier DT. Purkinje cell degeneration elevates eupneic and hypercapnic ventilation in rats. Cerebellum. 2004; 3(3):133–40. [PubMed: 15543803]
47. Tolbert D, Ewald M, Gutting J, La Regina M. Spatial and temporal pattern of Purkinje cell degeneration in shaker mutant rats with hereditary cerebellar ataxia. J Comp Neurol. 1995; 355(4): 490–507. [PubMed: 7636028]
48. Hartmann N, Martrette JM, Westphal A. Influence of the Lurcher mutation on myosin heavy chain expression in skeletal and cardiac muscles. J Cell Biochem. 2001; 81(S36):222–31.
49. Hernandez JP, Xu F, Frazier DT. Medial vestibular nucleus mediates the cardiorespiratory responses to fastigial nuclear activation and hypercapnia. J Appl Physiol. 2004; 97(3):835–42. [PubMed: 15333625]
50. Martino P, Davis S, Opansky C, Krause K, Bonis J, Pan L, et al. The cerebellar fastigial nucleus contributes to CO2-H+ ventilatory sensitivity in awake goats. Respir Physiol Neurobiol. 2007; 157(2):242–51. [PubMed: 17336598]
51. Mai, JK.; Paxinos, G. The human nervous system. Academic Press; 2011.
52. Heckroth JA. Quantitative morphological analysis of the cerebellar nuclei in normal and Lurcher mutant mice. I. Morphology and cell number. J Comp Neurol. 1994; 343(1):173–82. [PubMed: 8027434]
53. Koziol LF, Budding D, Andreasen N, D'Arrigo S, Bulgheroni S, Imamizu H, et al. Consensus paper: The cerebellum's role in movement and cognition. Cerebellum. 2014; 13(1):151–177. [PubMed: 23996631]
54. Kiessling MC, Büttner A, Butti C, Müller-Starck J, Milz S, Hof PR, et al. Intact numbers of cerebellar Purkinje and granule cells in sudden infant death syndrome: a stereologic analysis and critical review of neuropathologic evidence. J Neuropathol Exp Neurol. 2013; 72(9):861–70. [PubMed: 23965745]
55. Oehmichen M, Wullen B, Zilles K, Saternus K-S. Cytological investigations on the cerebellar cortex of sudden infant death victims. Acta Neuropathol. 1989; 78(4):404–9. [PubMed: 2782051]
56. Kaur C, Sivakumar V, Zou Z, Ling E-A. Microglia-derived proinflammatory cytokines tumor necrosis factor-alpha and interleukin-1beta induce Purkinje neuronal apoptosis via their receptors in hypoxic neonatal rat brain. Brain Struct Funct. 2014; 219(1):151–70. [PubMed: 23262920]

57. Yue X, Mehmet H, Penrice J, Cooper C, Cady E, Wyatt J, et al. Apoptosis and necrosis in the newborn piglet brain following transient cerebral hypoxia–ischaemia. Neuropathol Appl Neurobiol. 1997; 23(1):16–25. [PubMed: 9061686]
58. Welsh JP, Yuen G, Placantonakis DG, Vu TQ, Haiss F, O'Hearn E, et al. Why do Purkinje cells die so easily after global brain ischemia? Aldolase C, EAAT4, and the cerebellar contribution to posthypoxic myoclonus. Adv Neurol. 2001; 89:331–59. [PubMed: 11968459]
59. Kijsirichareanchai K, Limsuwat C, Mankongpaisarnrung C, Nantsupawat N, Nugent K. Chiari syndrome and respiratory failure: a literature review. J Intensive Care Med. 2013 doi: 10.1177/0885066613485213.
60. Maria BL, Boltshauser E, Palmer SC, Tran TX. Clinical Features and Revised Diagnostic Criteria in Joubert Syndrome. J Child Neurol. 1999; 14(9):583–90. doi: 10.1177/088307389901400906. [PubMed: 10488903]
61. Parsons LM, Egan G, Liotti M, Brannan S, Denton D, Shade R, et al. Neuroimaging evidence implicating cerebellum in the experience of hypercapnia and hunger for air. Proc Natl Acad Sci U S A. 2001; 98(4):2041–6. [PubMed: 11172072]
62. Peiffer C, Poline J-B, Thivard L, Aubier M, SAMSON Y. Neural substrates for the perception of acutely induced dyspnea. Am J Respir Crit Care Med. 2001; 163(4):951–7. [PubMed: 11282772]
63. Evans KC, Banzett RB, Adams L, McKay L, Frackowiak RS, Corfield DR. Bold fMRI identifies limbic, paralimbic, and cerebellar activation during air hunger. J Neurophysiol. 2002; 88(3):1500–11. [PubMed: 12205170]
64. Moruzzi G. Paleocerebellar inhibition of vasomotor and respiratory carotid sinus reflexes. J Neurophysiol. 1940; 3:20–32.
65. Kumar R, Macey PM, Woo MA, Alger JR, Harper RM. Diffusion tensor imaging demonstrates brainstem and cerebellar abnormalities in congenital central hypoventilation syndrome. Pediatr Res. 2008; 64(3):275–80. [PubMed: 18458651]
66. Sabaratnam M. Pathological and neuropathological findings in two males with fragile-X syndrome. J Intellect Disabil Res. 2000; 44(1):81–5. [PubMed: 10711653]
67. Fryns JP, Moerman P, Gilis F, d'Espallier L, Berghe HVD. Suggestively increased rate of infant death in children of fra (X) positive mothers. Am J Med Genet. 1988; 30(1-2):73–5. [PubMed: 3177481]
68. Limperopoulos C, Chilingaryan G, Sullivan N, Guizard N, Robertson RL, du Plessis AJ. Injury to the premature cerebellum: outcome is related to remote cortical development. Cereb Cortex. 2012:bhs354.
69. Bolduc ME, Du Plessis AJ, Sullivan N, Khwaja OS, Zhang X, Barnes K, et al. Spectrum of neurodevelopmental disabilities in children with cerebellar malformations. Dev Med Child Neurol. 2011; 53(5):409–16. [PubMed: 21418200]
70. Whitney ER, Kemper TL, Rosene DL, Bauman ML, Blatt GJ. Density of cerebellar basket and stellate cells in autism: evidence for a late developmental loss of Purkinje cells. J Neurosci Res. 2009; 87(10):2245–54. [PubMed: 19301429]
71. DiCicco-Bloom E, Lord C, Zwaigenbaum L, Courchesne E, Dager SR, Schmitz C, et al. The developmental neurobiology of autism spectrum disorder. J Neurosci. 2006; 26(26):6897–906. [PubMed: 16807320]
72. Palmen SJ, van Engeland H, Hof PR, Schmitz C. Neuropathological findings in autism. Brain. 2004; 127:2572–83. Pt 12. doi: 10.1093/brain/awh287. [PubMed: 15329353]
73. Courchesne E. Brainstem, cerebellar and limbic neuroanatomical abnormalities in autism. Curr Opin Neurobiol. 1997; 7(2):269–78. [PubMed: 9142760]
74. Courchesne E, Saitoh O, Yeung-Courchesne R, Press G, Lincoln A, Haas R, et al. Abnormality of cerebellar vermian lobules VI and VII in patients with infantile autism: identification of hypoplastic and hyperplastic subgroups with MR imaging. AJR Am J Roentgenol. 1994; 162(1): 123–30. [PubMed: 8273650]
75. Courchesne E, Yeung-Courchesne R, Hesselink J, Jernigan T. Hypoplasia of cerebellar vermal lobules VI and VII in autism. N Engl J Med. 1988; 318(21):1349–54. [PubMed: 3367935]
76. Bauman M, Kemper TL. Histoanatomic observations of the brain in early infantile autism. Neurology. 1985; 35(6):866. [PubMed: 4000488]

77. Ishikawa T, Zhu BL, Li DR, Zhao D, Michiue T, Maeda H. An autopsy case of an infant with Joubert syndrome who died unexpectedly and a review of the literature. Forensic Sci Int. 2008; 179(2-3):e67–73. doi: 10.1016/j.forsciint.2008.06.003. [PubMed: 18639400]

78. Lioy DT, Wu WW, Bissonnette JM. Autonomic dysfunction with mutations in the gene that encodes methyl-CpG-binding protein 2: Insights into Rett syndrome. Auton Neurosci. 2011; 161(1):55–62. [PubMed: 21316312]

79. Taddeucci G, Bonuccelli A, Mantellassi I, Orsini A, Tarantino E. Pitt-Hopkins syndrome: report of a case with a TCF4 gene mutation. Ital J Pediatr. 2010; 36(1):12. [PubMed: 20205897]

80. Miano S, Bruni O, Elia M, Musumeci SA, Verrillo E, Ferri R. Sleep breathing and periodic leg movement pattern in Angelman syndrome: a polysomnographic study. Clin Neurophysiol. 2005; 116(11):2685–92. [PubMed: 16213786]

81. Gilmore RL, Falace P, Kanga J, Baumann R. Sleep-disordered breathing in Möbius syndrome. J Child Neurol. 1991; 6(1):73–7. [PubMed: 2002206]

82. Schulte F, Kaiser H, Engelbart S, Bell E, Castell R, Lenard H. Sleep patterns in hyperphenylalaninemia: a lesson on serotonin to be learned from phenylketonuria. Pediatr Res. 1973; 7(6):588–99. [PubMed: 4350781]

83. Kornguth S, Gilbert-Barness E, Langer E, Hegstrand L. Golgi-Kopsch silver study of the brain of a patient with untreated phenylketonuria, seizures, and cortical blindness. Am J Med Genet. 1992; 44(4):443–8. [PubMed: 1442885]

84. Yachnis AT, Rorke LB. Cerebellar and brainstem development: an overview in relation to Joubert syndrome. J Child Neurol. 1999; 14(9):570–3. [PubMed: 10488901]

85. Jay V, Becker LE, Chan F, Perry TL. Puppet-like syndrome of Angelman A pathologic and neurochemical study. Neurology. 1991; 41(3):416. [PubMed: 2006012]

86. Murakami JW, Courchesne E, Haas R, Press G, Yeung-Courchesne R. Cerebellar and cerebral abnormalities in Rett syndrome: a quantitative MR analysis. AJR Am J Roentgenol. 1992; 159(1): 177–83. [PubMed: 1609693]

87. Oldfors A, Sourander P, Armstrong DL, Percy AK, Witt-Engerström I, Hagberg BA. Rett syndrome: cerebellar pathology. Pediatr Neurol. 1990; 6(5):310–4. [PubMed: 2242172]

88. Lengyel D, Zaunbauer W, Keller E, Gottlob I. Mobius syndrome: MRI findings in three cases. J Pediatr Ophthalmol Strabismus. 1999; 37(5):305–8. [PubMed: 11020114]

89. Nardelli E, Vio M, Ghersini L, Rizzuto N. Möbius-like syndrome due to multiple cerebral abnormalities including hypoplasia of the descending tracts. J Neurol. 1982; 227(1):11–9. [PubMed: 6176689]

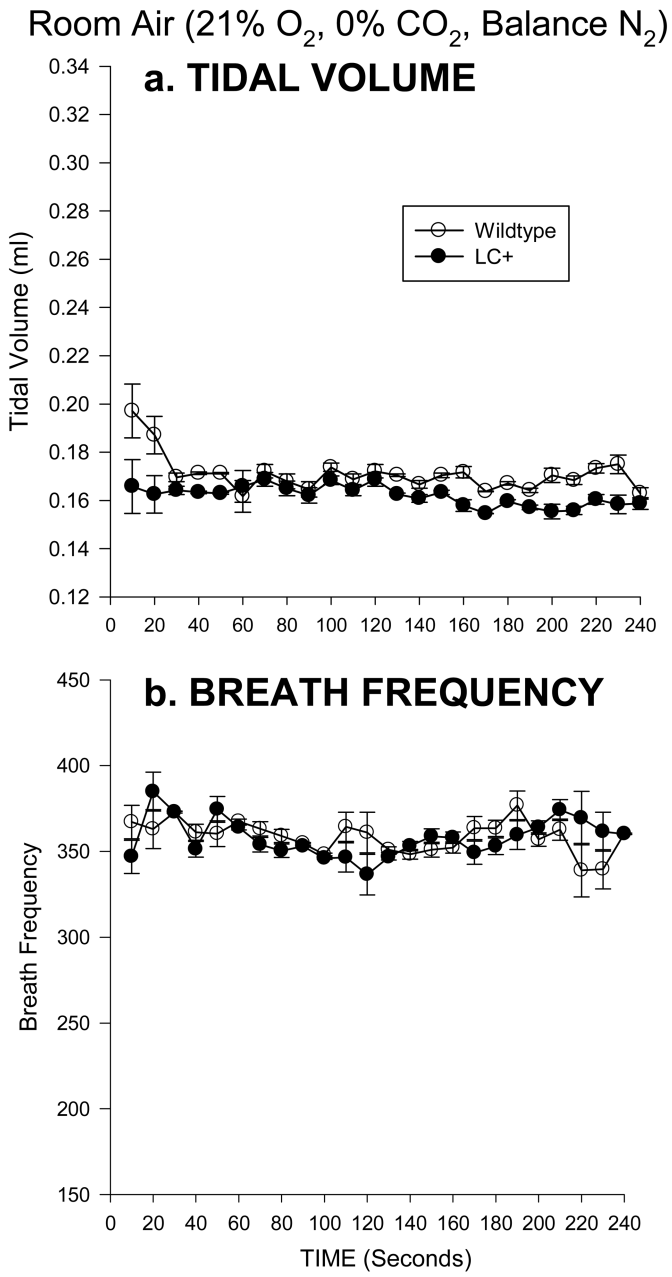

Fig 1.

Baseline ventilatory data over twenty four, 10 s intervals at normal room air (21% O_2, 0% CO_2, Balance N_2) in *Lurcher* mutant (LC+) and wildtype control mice. Values represent Mean ± SEM.

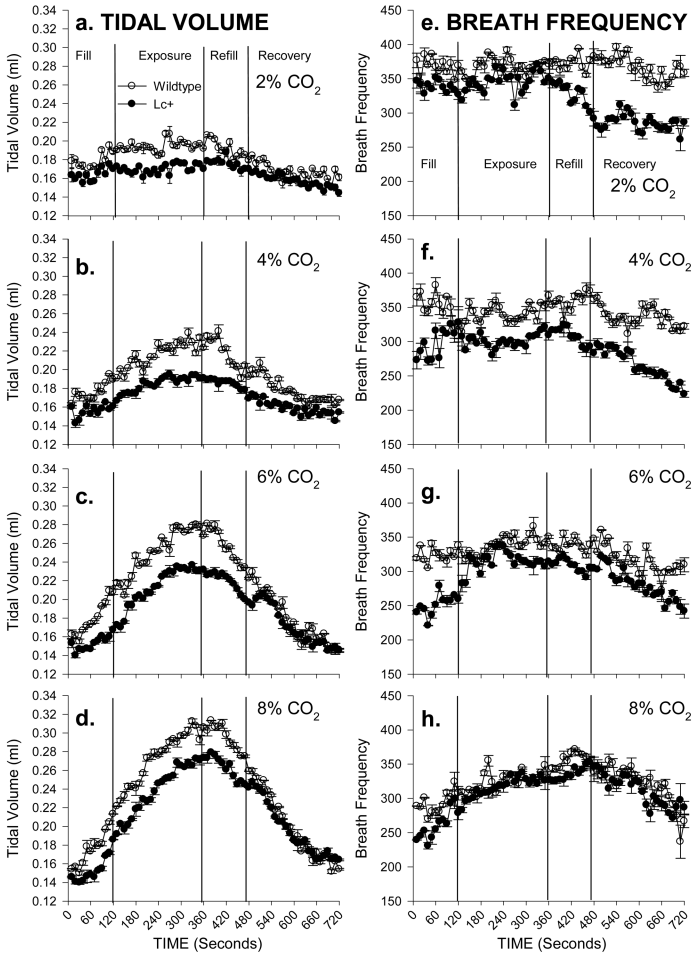

Fig 2.

Tidal volume and breath frequency in response to increasing concentrations of CO_2 (percentages indicated in the upper right corner of each panel figure). The horizontal axis in each figure depicts time intervals across 4 time blocks that correspond to chamber **Fill** with CO_2, **Exposure** to increased levels of CO_2, chamber **Refill** with room air and **Recovery** with room air maintained. Exposure and Recovery conditions were additionally subdivided into two, two-minute blocks (e.g. Exposure 1 & 2) for the purposes of statistical analyses. The vertical lines indicate the SEM.

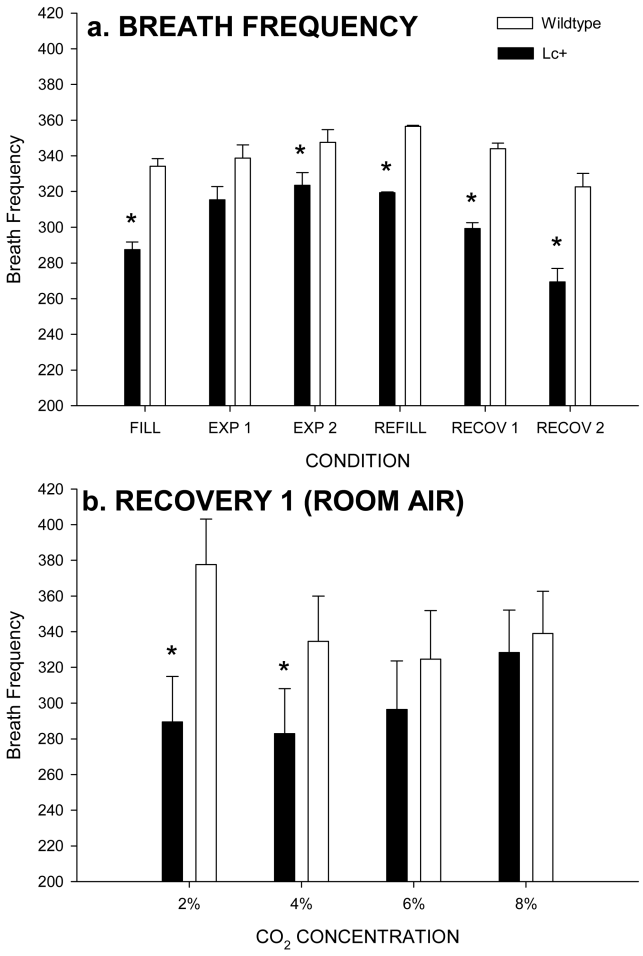

Fig 3.

(a) Genotypic differences in breath frequency among the six time blocks collapsed across all CO_2 challenges. **FILL** = chamber fill with CO_2 (2, 4, 6, & 8%), **EXP 1** = the first two minutes of gas exposure, **EXP 2** = the second two minutes of gas exposure, REFILL = chamber fill to normal room air, **RECOV 1** = the first two minutes of recovery, **RECOV 2** = the final two minutes of recovery. (**b**) Genotypic differences in in breath frequency when mice were re-exposed to room air following each CO_2 challenge. The vertical lines indicate the SEM.

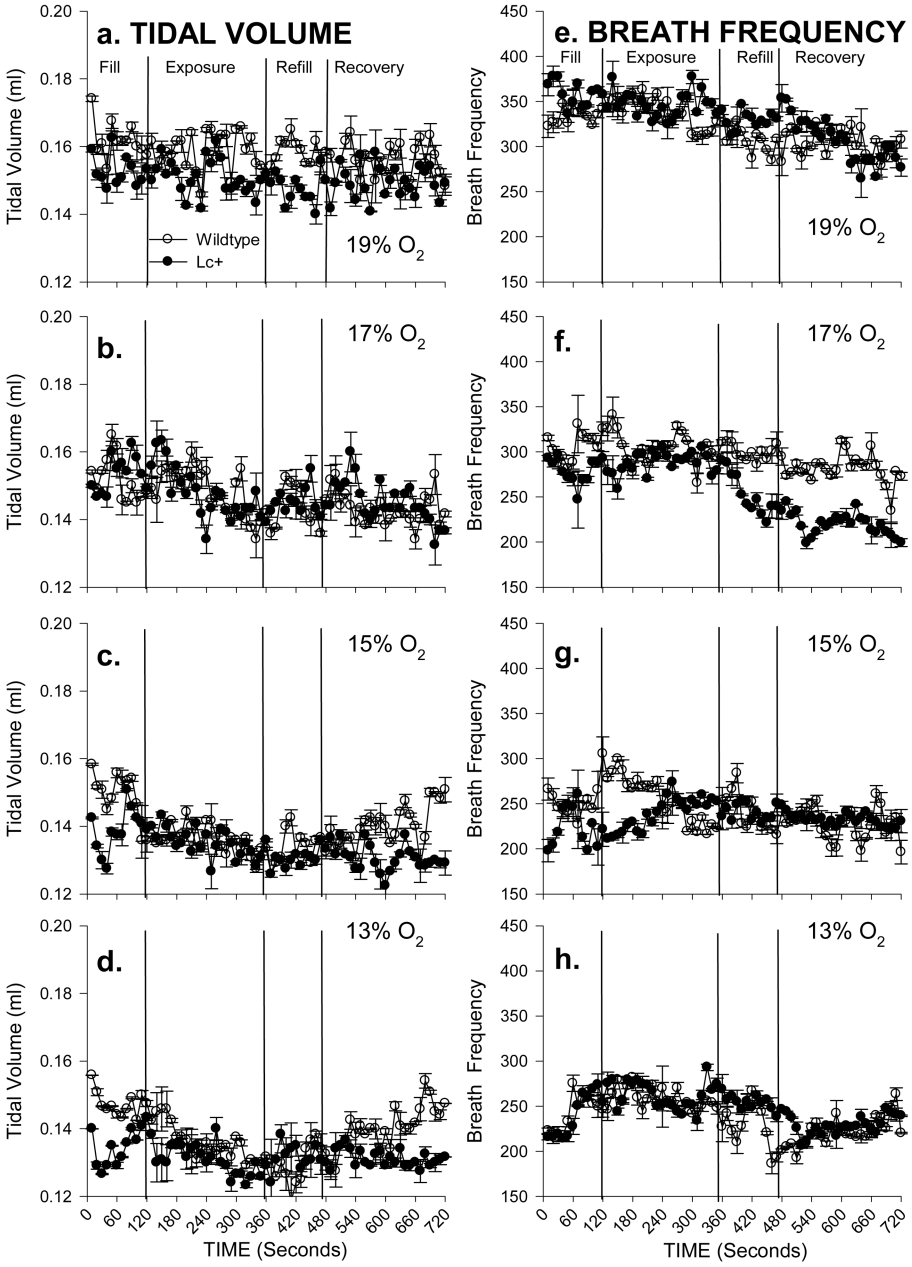

Fig 4.

Tidal volume and breath frequency in response to decreasing concentrations of O_2 (percentages indicated in the upper right corner of each panel figure). The horizontal axis in each figure depicts time intervals across 4 time blocks that correspond to chamber **Fill** with reduced concentration of O_2, **Exposure** to reduced levels of O_2, chamber **Refill** with room air and **Recovery** with room air maintained. Exposure and Recovery conditions were additionally subdivided into two, two-minute blocks (e.g. Exposure 1 & 2) for the purposes of statistical analyses. The vertical lines indicate the SEM. Note the y-axis change from Figure 2.